

# Integrated analysis of DNA methylation and mRNA expression profiles to identify key genes involved in the regrowth of clinically non-functioning pituitary adenoma

Sen Cheng<sup>1</sup>, Chuzhong Li<sup>2</sup>, Weiyan Xie<sup>1</sup>, Yazhou Miao<sup>1</sup>, Jing Guo<sup>1</sup>, Jichao Wang<sup>3</sup>, Yazhuo Zhang<sup>2</sup>

<sup>1</sup>Beijing Neurosurgical Institute, Capital Medical University, Beijing 100070, China

<sup>2</sup>Beijing Neurosurgical Institute, Beijing Tiantan Hospital Affiliated to Capital Medical University, Beijing Institute for Brain Disorders Brain Tumour Center, China National Clinical Research Center for Neurological Diseases, Key Laboratory of Central Nervous System Injury Research, Beijing 100070, China

<sup>3</sup>People's Hospital of Xin Jiang Uygur Autonomous Region, Urumqi 830001, China

**Correspondence to:** Yazhuo Zhang; email: [zyz2004520@yeah.net](mailto:zyz2004520@yeah.net)

**Keywords:** clinically non-functioning pituitary adenoma, DNA methylation, regrowth prediction

**Received:** September 26, 2019

**Accepted:** January 7, 2020

**Published:** February 3, 2020

**Copyright:** Cheng et al. This is an open-access article distributed under the terms of the Creative Commons Attribution License (CC BY 3.0), which permits unrestricted use, distribution, and reproduction in any medium, provided the original author and source are credited.

## ABSTRACT

Tumour regrowth is a key characteristic of clinically non-functioning pituitary adenoma (NFPA). No applicable prognosis evaluation method is available for post-operative patients. We aimed to identify DNA methylation biomarkers that can facilitate prognosis evaluation. Genome-wide DNA methylation and mRNA microarray analyses were performed for tumour samples from 71 NFPA patients. Differentially expressed genes and methylated genes were identified based on the regrowth vs non-regrowth grouping. There were 139 genes that showed alterations in methylation status and expression level, and only 13 genes showed a negative correlation. The progression-free analysis found that *FAM90A1*, *ETS2*, *STAT6*, *MYT1L*, *ING2* and *KCNK1* are related to tumour regrowth. A prognosis-prediction model was built based on all 13 genes from integrated analysis, and the 6-gene model achieved the best area under the receiver operating characteristic curves (AUC) of 0.820, compared with 0.785 and 0.568 for the 13-gene and 7-gene models, respectively. Our prognostic biomarkers were validated by pyrosequencing and RT-PCR. *FAM90A1* and *ING2* was found to be independent prognostic factors of tumour regrowth with univariate Cox regression. The DNA methylation and expression levels of *FAM90A1* and *ING2* are associated with tumour regrowth, and may serve as biomarkers for predicting the prognosis of patients with NFPA.

## INTRODUCTION

Pituitary adenoma (PA) is the third most common intracranial neoplasm [1]. PA arises from different anterior pituitary secretory cells and is therefore characterized by the over-secretion of certain hormones and causes relevant clinical symptoms. However, the largest subgroup of pituitary adenoma shows no specific serum hormone level change and mainly induces mass effects, including visual disturbance, headache and various degrees of hypopituitarism; this subgroup is called clinically non-functioning pituitary adenoma (NFPA) [2, 3].

Surgery has been suggested to be the most effective treatment for NFPA. However, approximately 12-58% of patients with macro-adenoma or giant adenoma will experience tumour regrowth within five years [4]. Compared with clinically functioning pituitary adenoma whose regrowth can be manifested by serum hormonal alteration, there is no practical approach to monitor the tumour regrowth of NFPA, except magnetic resonance imaging (MRI).

Interest in tumour epigenetic studies has attracted considerable attention in recent years. Epigenetic abnormalities, especially the aberrant DNA methylation,

are recognized as hallmarks of tumorigenesis and patients' prognosis [5–10]. Studies have shown that DNA methylation may play a pivotal role in pituitary adenoma tumorigenesis, but the alteration in DNA methylation of tumour regrowth has not been fully illustrated yet [11].

In this study, we used whole-genome DNA methylation and mRNA microarray analysis and identified thirteen genes that showed differential DNA methylation and expression levels. We then established a regrowth prediction model with six genes that was also valuable in progress-free survival (PFS) analyses. Two genes were found to be independent prognostic factor of NFPA regrowth. We aimed to identify efficient DNA

methylation and expression parameters to evaluate the regrowth of NFPA.

## RESULTS

### Identification of differentially methylated genes (DMGs)

The flowchart of the study is shown in Figure 1. Based on the criteria mentioned above, we divided all patients into regrowth and non-regrowth groups. The summary of clinical characteristics of these 71 patients (20 regrowth and 51 non-regrowth patients) are shown in Table 1 and detailed information is provided in Supplementary Table 1. We compared the

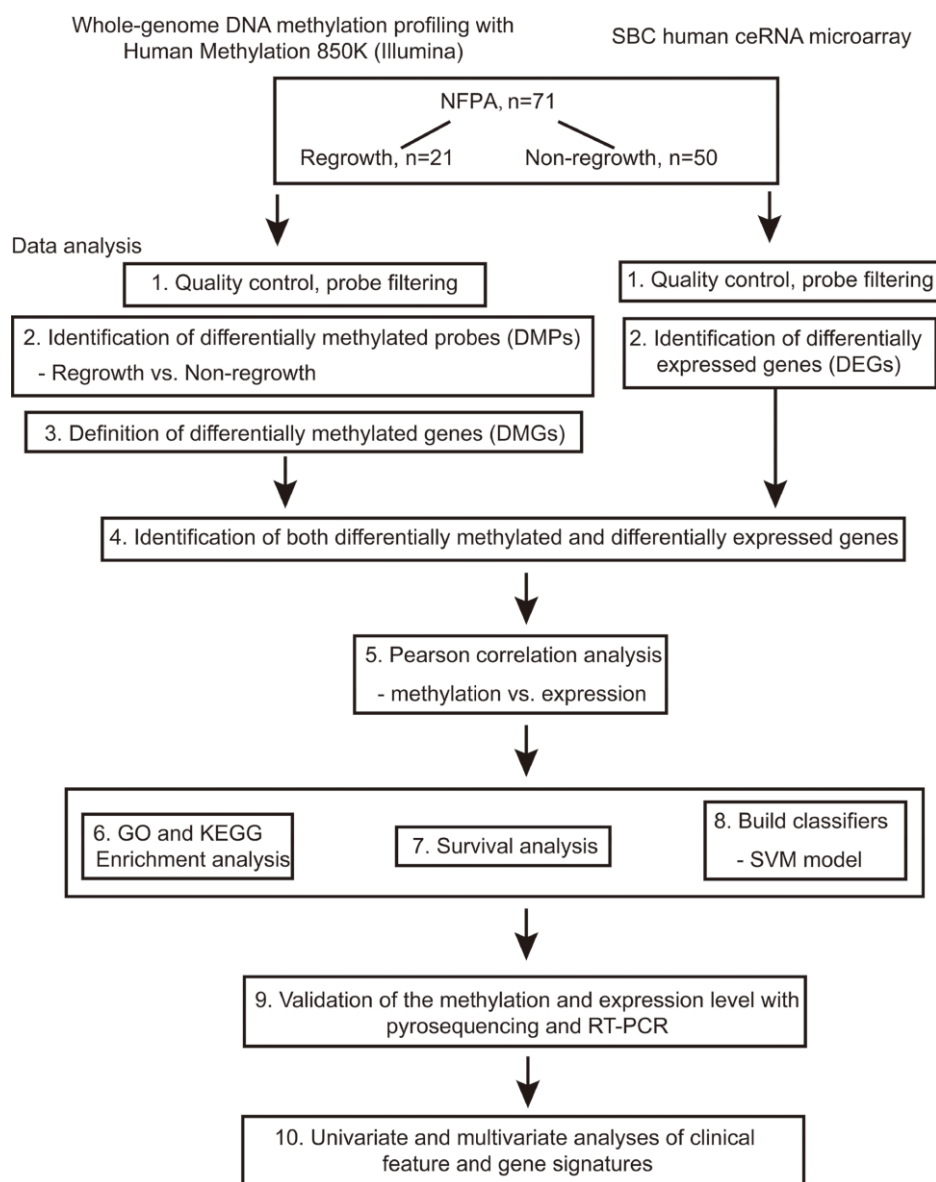


Figure 1. Flowchart of this study.

**Table 1. Clinical characteristics of 71 patients with NFPA.**

	N	Percentage
<b>Gender</b>		
Male	36	50.7%
Female	35	49.3%
<b>Age</b>		
Mean	50.45±11.7	
Median	52	
<b>Tumour Volume</b>		
Macro-	51	71.8%
Giant	20	28.2%
<b>Invasive</b>		
Yes	39	54.9%
No	32	45.1%
<b>Subtype</b>		
Null cell	49	69.0%
Gonadotroph	22	31.0%
<b>Resection</b>		
GTR	35	49.3%
NGTR	36	50.7%

Abbreviations: Macro, macro-adenoma (1-4 cm); Giant, giant adenoma (>4cm); GTR, gross total resection; NGTR, non-gross total resection.

DNA patterns in the two groups by high-throughput DNA methylation screening. After filtering the raw data and statistical analysis, we determined that 6636 CpG sites in promoter region which are related to 3329 different genes showing significant differences in promoter DNA methylation status between regrowth and non-regrowth patients, of which, 2788 genes were found to be hypomethylated and 541 genes were hypermethylated in regrowth group (Figure 2A and Supplementary Table 2). The heatmap showed the methylation status of these genes based on beta values of these CpG sites across all 71 samples ( $p < 0.05$ ,  $|\Delta\beta| > 0.1$ , Figure 2B).

#### Identification of differentially expressed genes (DEGs)

We measured the expression levels of 18854 genes between regrowth and non-regrowth patients. Five hundred one genes were differentially expressed ( $p < 0.05$ , fold change  $> 1.5$  or  $< 0.67$ ) between two groups, of which 63 genes were found to be upregulated and 438 genes were downregulated in regrowth group (Figure 2C and Supplementary Table 3). The heatmap and volcano plot of the DEGs are presented in Figure 2D.

#### Integrated analysis of DMGs and DEGs

We only focused on genes that showed both expression changes and methylation alteration. To this

end, 139 of the 501 genes are both differentially promoter methylated and expressed (Figure 3A). The enrichment analysis showed that these genes are tumour related, such as cell adhesion, apoptotic process, signal transduction, extracellular region, and pathways in cancer (Figure 3B and Supplementary Table 5).

We further studied the correlation of 139 genes' promoter methylation status and expression state by Pearson correlation analysis. Then, 13 genes (cytochrome b reductase 1 [*CYBRD1*], endoplasmic reticulum-to-nucleus signaling 1 [*ERN1*], ETS proto-oncogene 2 [*ETS2*], family with sequence similarity 90 member A1 [*FAM90A1*], hes related family bHLH transcription factor with YRPW motif 1 [*HEY1*], inhibitor of growth family member 2 [*ING2*], potassium two pore domain channel subfamily K member 1 [*KCNK1*], matrix metalloproteinase 14 [*MMP14*], myelin transcription factor 1-like [*MYT1L*], *PYD* and CARD domain containing [*PYCARD*], SH3 domain containing GRB2-like 2, endophilin A1 [*SH3GL2*], signal transducer and activator of transcription 6 [*STAT6*], ubiquitin specific peptidase 31 [*USP31*]) with negative correlation between DNA methylation and expression level were selected ( $p < 0.05$ ,  $R < -0.2$ , Figure 3C and Supplementary Table 4). Enrichment analysis of these 13 genes also showed the relevance of tumour oncogenesis. (Figure 3D and Supplementary Table 6).

## Discovering candidate regrowth biomarkers in NFPA

Meanwhile, in order to assess the associations between gene expression level and time-to-event, we performed PFS analyses to further confirm whether there are possible candidates. The event endpoint was calculated from surgical resection to the date of the first regrowth. Patients were divided into 2 groups, a low-expression group and a high-expression group, according to the median cut-off of the gene expression levels. Our results indicated that patients with the over-expression of *FAM90A1*, *ETS2* and *STAT6* were less prone to face with regrowth, whereas the over-expression of *MYTIL*, *ING2* and *KCNK1* was correlated with poor prognosis (Figure 4). The expression levels of the other 7 genes were not

significantly related to clinical outcome of NFPA (Supplementary Figure 1).

## Identification of potential regrowth predictive biomarkers in NFPA

Based on the above observations, these 6 of 13 genes (*FAM90A1*, *ETS2*, *STAT6*, *MYTIL*, *ING2* and *KCNK1*) were considered as potential biomarkers associated with the regrowth of NFPA. To further investigate whether these 6 genes could efficiently distinguish regrowth patients from non-regrowth patients, we performed unsupervised hierarchical clustering for 71 samples in the cohort according to the expression pattern of 6-gene biomarkers. We integrated these 6 genes to construct a 6-gene signature by developing a support vector machine (SVM) model.

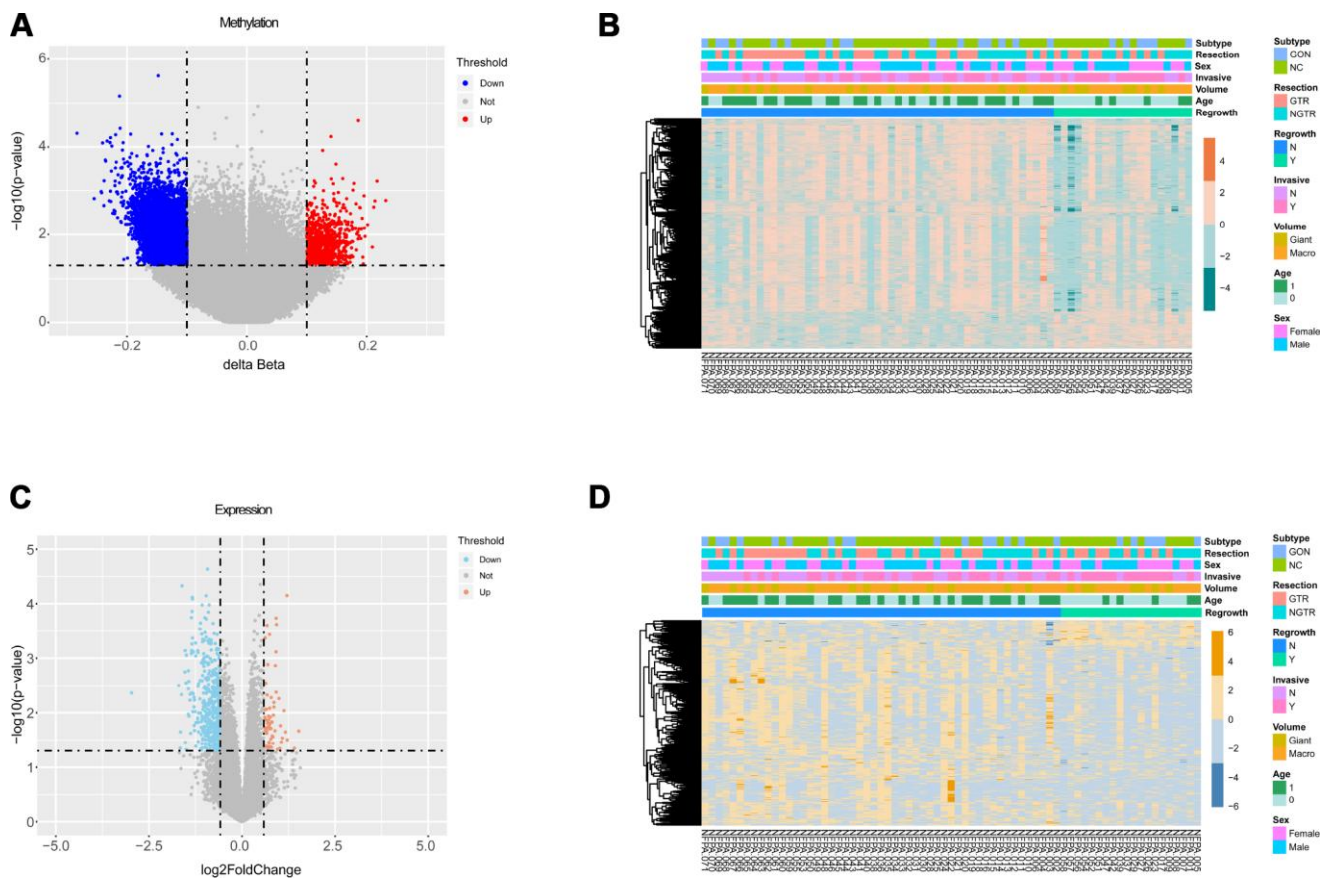


**Figure 2. Differential analyses of gene methylation and expression status between regrowth and non-regrowth patients. (A)** There are 3329 differentially methylated genes, of which 2788 hypomethylated genes (blue) and 541 hypermethylated genes (red) **(B)** The heatmap shows methylation profiles of 71 NFPA samples. The rows represent the different probes, and the columns represent each sample. The color in the heatmap represents the methylation level difference, which are hypermethylation (orange) and hypomethylation (green). The bar on the top shows the clinical and grouping information, and the sample ID is on the bottom. **(C)** The volcano plot shows 501 differentially expressed genes, and there are 438 upregulated genes (red) and 63 downregulated genes (blue). **(D)** The heatmap shows the expression profiles of the 71 NFPA samples. The rows represent the different genes, and the columns represent each sample. The color in the heatmap represents the expression level difference: upregulated (yellow) and downregulated (blue). The bar on the top shows the clinical and grouping information, and the sample ID is on the bottom.

The performance of the model was evaluated in this cohort using the leave one out cross-validation (LOOCV) procedure, in which 70 samples were used as training set and the remaining one was served as the test sample. The results of the cohort showed that the model was able to correctly classify 20 out of 71 samples, achieving an overall predictive accuracy of 83.1%. The discriminatory performance of the model, evaluated by calculating the AUC, revealed that the AUC was 0.820, which was significantly higher than those of randomization tests (Figure 5A).

Meanwhile, we also construct a 13-gene signature and a 7-gene (except the 6 genes selected from 13 genes)

signature by developing an SVM model. The performance of these models was evaluated in the same cohort using the LOOCV procedure. Our results showed that the 13-gene model was able to correctly classify 20 out of 71 samples, achieving an overall predictive accuracy of 80% with an AUC of 0.785, which were significantly higher than those of randomization tests (Figure 5B). Additionally, the 7-gene model was unable to correctly classify 20 out of 71 samples with an overall predictive accuracy of 59% with an AUC of 0.568, which were almost the same with those of randomization tests (Figure 5C). Our results demonstrated that the 6-gene model had better predictive performance for discriminating regrowth patients from non-regrowth patients.

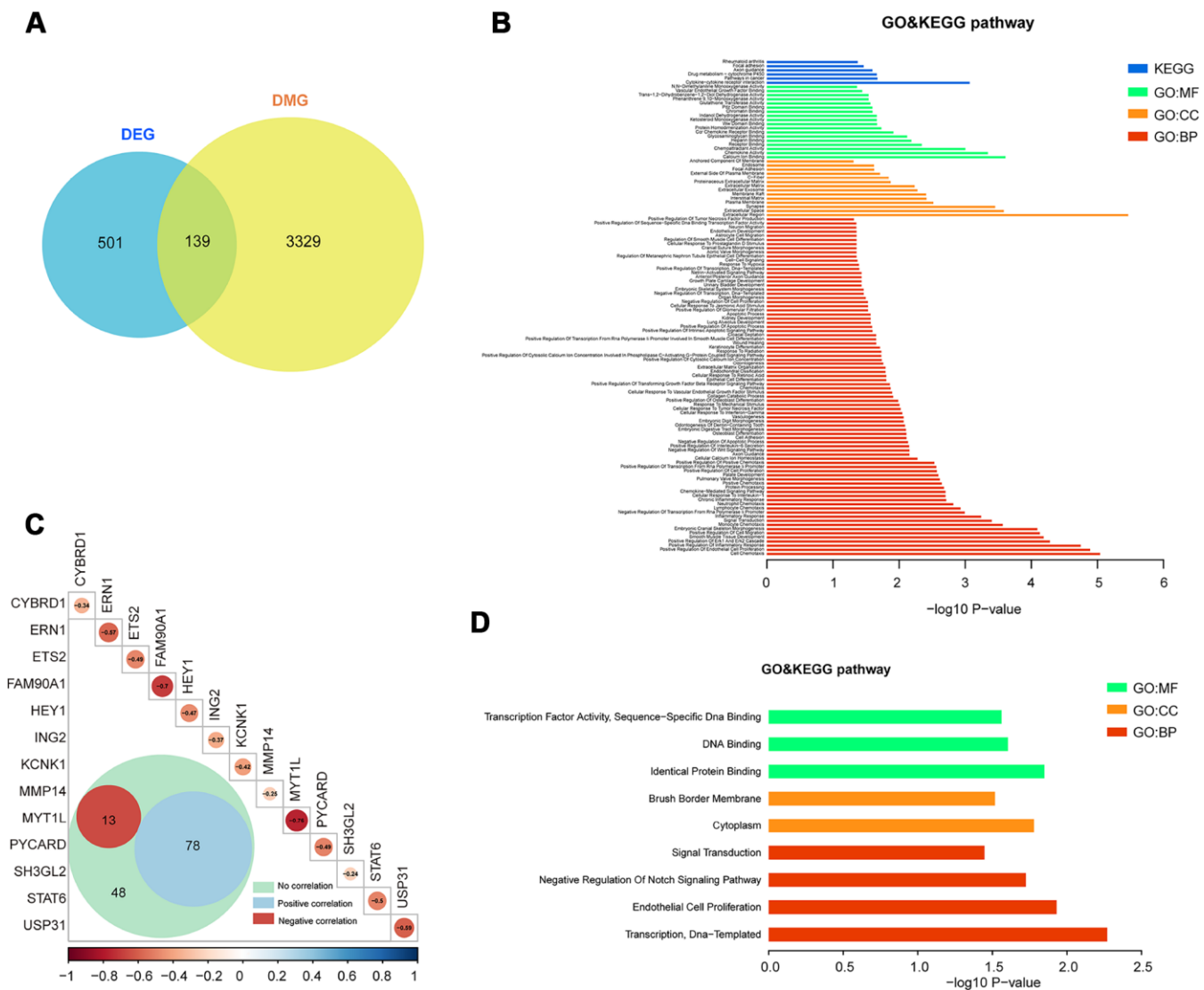


**Figure 3. Integrated analysis of DMGs and DEGs.** (A) The Venn diagram shows 139 genes with both DNA methylation and expression level changes. (B) GO and KEGG pathway analyses of 139 genes. (C) Pearson analysis of 139 genes. There are 13 genes showing negative correlation (red), 78 genes showing positive correlation (blue) and 48 genes showing no correlation. The R value of 13 genes is shown. (D) GO and KEGG pathway analyses of 13 negative correlation genes.

## Validation of the DNA methylation and expression levels of the candidate predictive biomarkers

To further determine the authenticity of the DNA methylation level of the 13 gene signatures, pyrosequencing was performed in an additional set of patients based on the DMGs analyses. A significant increase of DNA methylation level in the regrowth group

compared with non-regrowth group was observed in *FAM90A1*, *ETS2*, *STAT6*, *CYBRD1* and *PYCARD* (Figure 6A, 6G, 6M, Supplementary Figures 2A and 3A). Decreased methylation levels were observed in *MYT1L*, *ING2*, *KCNK1* and *SH3GL2* (Figure 6D, 6J, 6P and Supplementary Figure 3D). Conversely, no significant DNA methylation change was found in *ERNI*, *HEY1*, *MMP14*, *USP31* (Supplementary Figure 2C, 2E, 2G 2I).

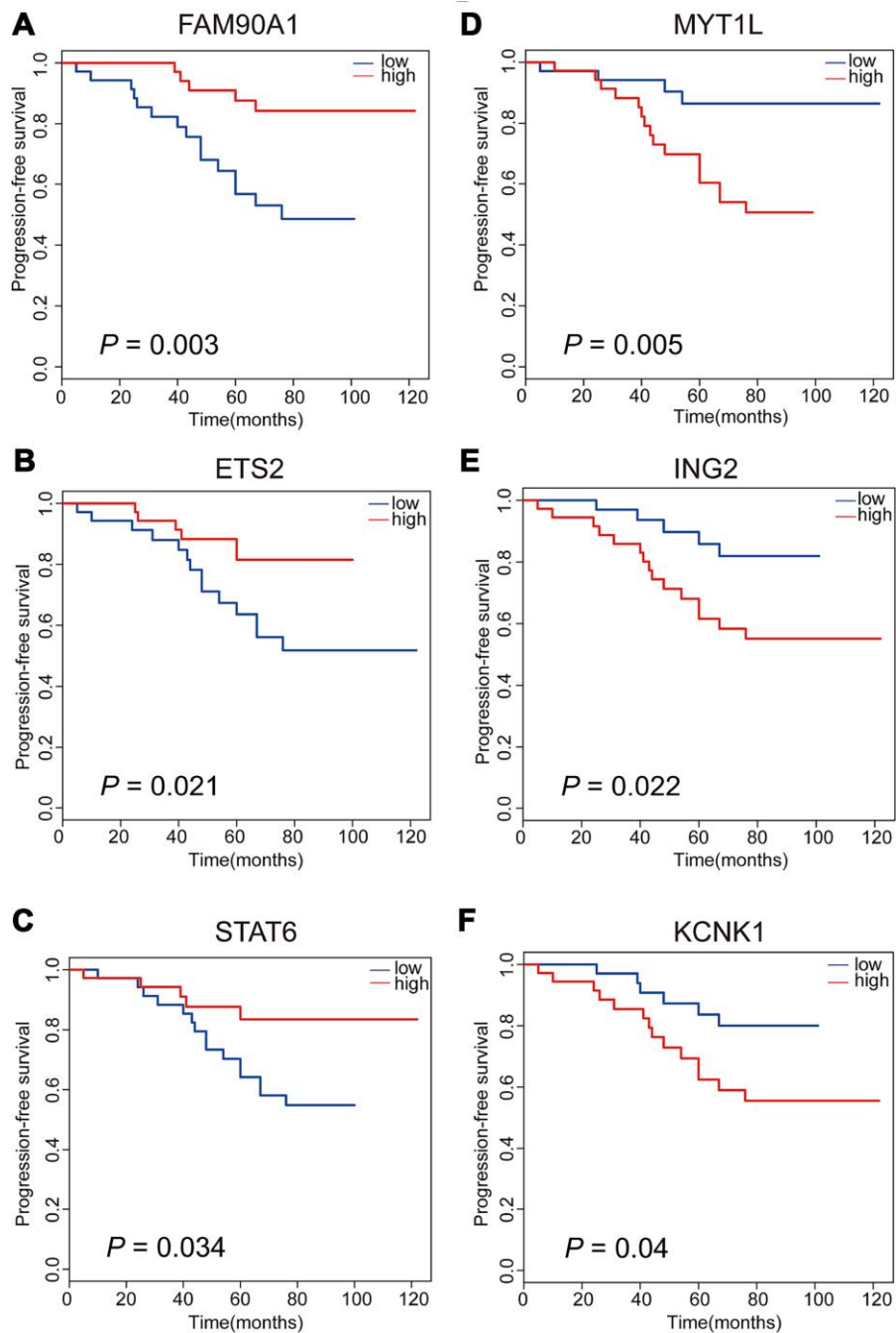


**Figure 4. Kaplan-Meier analyses of six significant genes in patients with NFPA.** Patients with upregulation of *FAM90A1*, *ETS2* and *STAT6* are less likely to have tumour regrowth (A–C). Patients with downregulation of *MYT1L*, *ING2* and *KCNK1* are less likely to have tumour regrowth (D–F).

Gene expression levels of 13 genes were assessed by RT-PCR in the same tumour samples that were used for pyrosequencing. We found a significant decrease in the expression level between the regrowth and non-regrowth groups in *FAM90A1*, *ETS2*, *STAT6*, *HEY1* and *PYCARD* (Figure 6B, 6H 6N, Supplementary Figures 2F and 3B). Increased expression levels were observed in *MYTIL*, *ING2*, *KCNK1*, *USP31* and *SH3GL2* (Figure 6E, 6K, 6Q, Supplementary Figures 2J and 3E). No significant expression change was found in *CYBRD1*, *ERN1* and *MMP14* (Supplementary Figure 2B, 2D, 2H).

Pearson analyses showed that the methylation status and expression levels of *FAM90A1*, *MYTIL*, *ETS2*, *ING2*, *STAT6*, *KCNK1*, *PYCARD*, *SH3GL2* showed a significantly negative correlation (Figure 6C, 6F, 6I, 6L, 6O, 6R and Supplementary Figure 3C, 3F).

These results confirmed that the methylation and expression levels of *FAM90A1*, *MYTIL*, *ETS2*, *ING2*,

*STAT6* and *KCNK1* were consistent with the DNA methylation and mRNA microarray analyses.

### Clinical features and gene signatures related with tumour regrowth of NFPA

We used Cox regression analysis to identify the independent prognostic factors from clinical parameters and gene signatures. Through univariate and multivariate cox regression analyses, we found patients with younger age (HR = 0.323, 95% CI = 0.121 to 0.863,  $p = 0.024$ ), decreased expression of *FAM90A1* (HR = 0.233, 95% CI = 0.083 to 0.649,  $p = 0.005$ ) and increased expression of *ING2* (HR = 3.020, 95% CI = 1.067 to 8.543,  $p = 0.037$ ) seems more likely to have tumour regrowth (Table 2). Age, expression of *FAM90A1* and *ING2* are independent prognostic factors of tumour regrowth. Our results showed that *FAM90A1* and *ING2* could be used as effective prognostic factors.

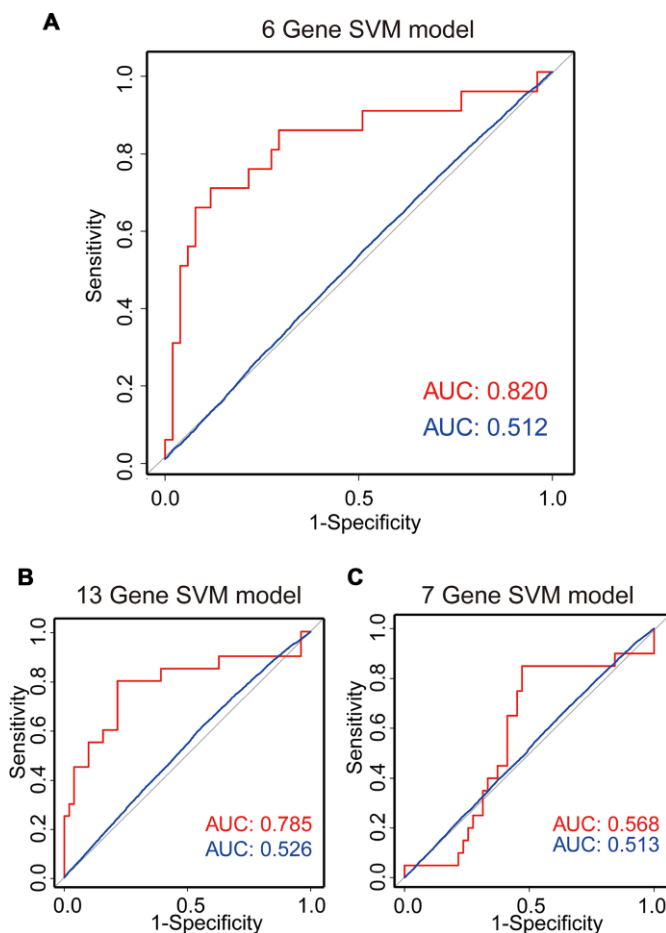


**Figure 5. SVM regrowth prediction model.** Three ROC curves using LOOCV show the comparisons of the AUC for the prediction of regrowth with 6 genes (A), 13 genes (B) and 7 genes (C). The red line shows the prediction model efficiency, and the blue line shows the permutation p-value of AUC was obtained from 1,000 randomization tests for testing the null hypothesis. The 6-gene model shows a better prediction accuracy.

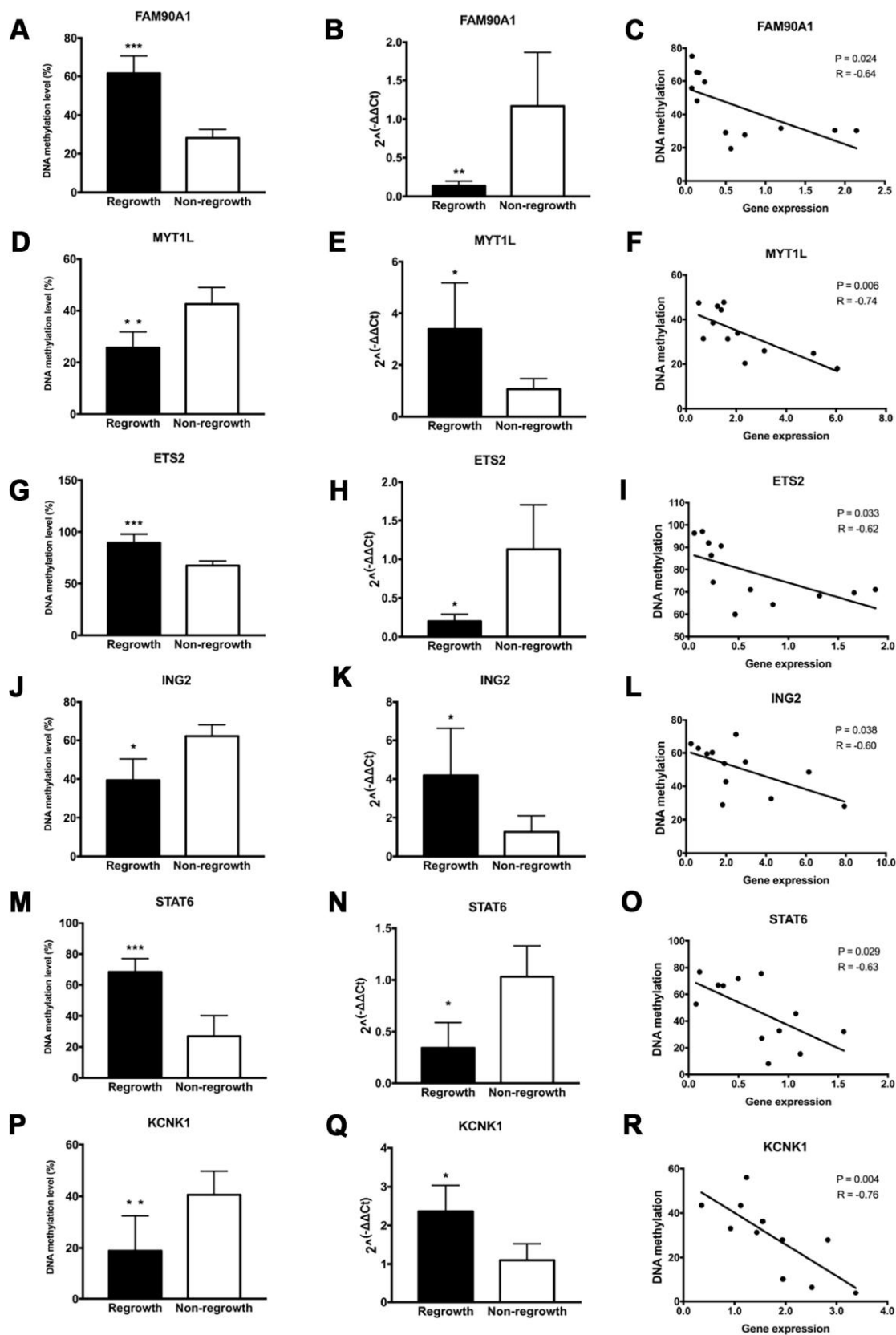


**Figure 6. Evaluation of DNA methylation and expression levels of selected genes.** The DNA methylation status, expression levels and Pearson correlation of FAM90A1, MYT1L, ETS2, ING2, STAT6, KCNK1 are shown. Each dot represents the average DNA methylation and gene expression level for every sample. \*  $p < 0.05$ , \*\*  $p < 0.01$ , \*\*\*  $p < 0.001$ .



**Table 2. Features related with tumour regrowth.**

Features	Univariate Cox regression		Multivariate Cox regression	
	HR (95%CI)	p value	HR (95%CI)	p value
Gender (Male vs Female)	0.809 (0.328-1.992)	0.644		
Age ( $\geq 50$ vs $< 50$ )	0.331 (0.126-0.872)	0.025	0.323 (0.121-0.863)	0.024
Volume (Giant vs Macro)	1.802 (0.648-5.013)	0.259		
Invasion (Invasive vs Non-invasive)	2.049 (0.804-5.222)	0.133		
Resection (Total vs Non-total)	0.898 (0.361-2.238)	0.818		
FAM90A1	0.278(0.100-0.775)	0.014	0.233(0.083-0.649)	0.005
MYT1L	3.023(1.088-8.395)	0.034	2.120(0.760-5.912)	0.151
ETS2	0.308(0.111-0.857)	0.024	0.526(0.173-1.596)	0.256
ING2	3.093(1.113-8.591)	0.03	3.020(1.067-8.543)	0.037
STAT6	0.411(0.148-1.140)	0.088		
KCNK1	1.936(0.762-4.919)	0.165		

Abbreviations: HR, hazard ratios; 95% CI, 95% confidence intervals; Macro, macro-adenoma; Giant, giant adenoma; Total, total resection; Non-total, non-total resection.

## DISCUSSION

Approximately 12%-58% patients with pituitary adenoma may face with tumour regrowth in 3-5 years [4]. For functioning pituitary adenoma, the changes in serum hormone levels and corresponding endocrine symptoms provide a feasible approach for regrowth evaluation. However, there is no specific endocrine symptoms in NFPA and it is mostly diagnosed and postoperatively monitored via imaging examinations. The chance of early intervention may have vanished when the symptoms of mass effect appear or when imaging examination shows tumour volume changes. For the above reasons, we attempt to identify efficient parameters to evaluate the regrowth of NFPA.

Although germline and somatic mutations are thought to be related to tumorigenesis of some types of pituitary adenoma, the drivers of NFPA is still unknown, as are the drivers of the regrowth of the tumour [12]. In the current field of NFPA, some genes have been reported to affect the prognosis of patients with NFPA and may be potentially used as prognostic biomarkers for NFPA. Ki-67 is commonly recognized as associated with regrowth of NFPA and high ki-67 index often indicates higher cell growth rate and shorter regrowth interval [13, 14]. Noh et al reported that high ki-67, PTTG1 as well as cell proliferation and apoptosis related genes, such as phospho-Akt, phospho-p44/42 MAPK, are related with tumour regrowth [15]. We have also tried to use known tumour-associated proteins and clinical factors to predict tumour regrowth and have obtained promising

results [16]. However, above studies have not taken all molecular markers that may cause tumour regrowth into discussion, so some important markers may be missed. Therefore, in this study we performed genome-wide methylation and transcriptomic analysis, and tried to study the factors related to tumour growth from a broader perspective. Also, targeting DNA methylation sites as prognostic biomarkers for NFPA has not been explored, and our study is the first to report DNA methylation signatures combining genetic parameters for the prognosis evaluation of NFPA patients.

In this study, potential prognostic biomarkers of NFPA were found in sites of DNA methylation and expression in tumours of patients with NFPA. Thirteen genes that showed concordance in gene methylation status and expression levels were selected to perform the prognosis analysis and six genes were found to be related to the regrowth of NFPA. Through prognostic analyses of clinical parameters and six genes, age, *FAM90A1* and *ING2* was found to be the independent factors of tumour regrowth. The DNA methylation and expression level of *FAM90A1* and *ING2* could serve as a new biomarkers for the early prognosis evaluation.

The use of Illumina Methylation 850K chip allowed a long list of aberrantly methylated CpGs to be identified. In combination with the mRNA microarray, we successfully recognized genes that may be regulated by DNA methylation. Several studies have identified that changes in DNA

methylation status were correlated with poor prognosis of patients with pituitary adenoma [17–19]. In this study, we identified 2 genes which can be used as independent risk factor of tumour regrowth. *FAM90A1* belongs to the family with sequence similarity 90 member, of which the encoding potential and function have not been fully illustrated but the variation in the organization and the number of copies of it is widely found in the human population [20, 21]. The methylation status of *FAM90A1* appeared to decrease mostly with age in postnatal development [22]. *ETS2* interacts with Pit-1-binding within the PRL promoter. It is able to mediate transcriptional responses to growth factors and activate the Ras/mitogenactivated protein kinase (MAPK) pathway to influence the secretion of several different hormones in functioning pituitary adenoma [23]. The upregulation of *ETS2* was found in acute myeloid leukaemia, prostate cancers, renal cell carcinoma and breast cancer, and it shows close correlation with poor prognosis [24–27]. In our study, we found that the methylation level of *ETS2* is higher in regrowth patients and that patients with upregulation of *ETS2* seem less likely to face with tumour regrowth. *ING2* is a member of the inhibitor of growth family, of which represents as a tumour suppressor [28]. *ING2* expression is usually decreased or lost in many human tumours, but another study found its expression to be upregulated [29–32]. However, The expression level and regulation mechanism has not been illustrated in pituitary adenoma. *KCNK1*, a member of the inwardly rectifying K<sup>+</sup> channel family, encodes TWIK-1, which is a part of potassium (K<sup>+</sup>) channels [33, 34]. We found the *KCNK1* gene upregulated in regrowth tumours, which may indicate a more active metabolism status. However, our results failed to illustrate the underlying mechanism within the methylation changes because we did not find the alterations of DNMT family, which are indispensable to *de novo* methylation and maintenance of methylation status [35, 36].

Clinical features such as age, gender, tumour volume and Knosp grade are widely accepted as factors that can affect the prognosis of patients with NFPA [4, 37–39]. The collection of information concerning these risk factors for NFPA regrowth is also of importance, which will provide valuable features and help to establish an effective prediction model. Because of limited sample size, number of patients in our study restricts us to evaluate the accuracy of our model in an additional validating set. However, our study is the first to try integrating DNA methylation signatures with genetic parameters for the prognosis of NFPA patients. Our further research intends to enlarge the patients' cohort and adjust our prediction

model to integrate with clinical parameters for future clinical practice.

There is another limitation of our study. We realize the importance of cell-based experiment, but we did not perform cell-based studies except pyrosequencing and RT-PCR for the following reasons. Firstly, there are no targeted methylated or demethylated drugs that could interfere the specific methylation sites, so it is impossible to specifically alter the methylation level of a gene like we interfere the gene expression using lentivirus, shRNA or siRNA. Also, there is no human or murine cell lines of NFPA. So far, the cell lines that is commonly used for research are murine cell lines of functioning pituitary adenomas. Therefore, we did not explore their functions here. But, we are trying to establish the human cell line, and we will study the function of these genes in further research.

In conclusion, this is the first study to integrated DNA methylation and gene expression in NFPA in order to effectively identify key genes underlying tumour regrowth. The DNA methylation and expression levels of *FAM90A1* and *ING2* may serve as biomarkers for predicting the prognosis of patients with NFPA. Our study may promote the prognosis evaluation and early intervention to patients with NFPA.

## MATERIALS AND METHODS

### Patients

We retrospectively collected regrowth and non-regrowth NFPA samples from 71 patients diagnosed with NFPA at Beijing Tiantan Hospital from October 2007 to July 2016. All patients were performed enhanced head MRI scans before and after surgery to assess the maximum tumour diameter, Knosp grade and tumour resection rate. The criteria of regrowth were defined as maximum tumour diameter increases more than 2 mm on enhanced MRI from the day of surgery to follow-up endpoint with or without the reappearance of visual disturbance, headache or hypopituitarism. The minimum follow-up time was 17 months, and the average follow-up time was 64.9 months (range, 17-126 months).

### Tissue sample preparation

All samples were obtained from the Beijing Tiantan Hospital, neurosurgical department. Tumour samples were immediately put into liquid nitrogen and stored at -196°C once they were resected from the sellar region. A total of 71 pituitary adenoma samples were included to perform methylation and mRNA microarray analysis.

## Whole genome DNA methylation microarray

Total DNA was isolated and purified using the DNeasy Blood and Tissue Kit (Cat#69504, QIAGEN, Germany). The bisulfite conversion of the tumour DNA was performed using an EZ DNA Methylation-Gold™ Kit (D5005, Zymo, USA). Illumina Infinium MethylationEPIC 850K BeadChip was used to analyze the total DNA methylation status of 71 NFPA samples. The DNA methylation microarray experiment was performed following the manufacturer's instructions of Illumina at Shanghai Biotechnology Corporation. Probes located on the X and Y chromosomes, associated with a known SNP or bound to multiple genomic locations were excluded. We also removed probes that failed to be detected above background. The bio-conductor R package *minfi* (v1.18.6) was used for quality control and normalization of the raw data. The methylation status of a CpG site was calculated with the mean-difference  $\beta$ -value ( $\Delta\beta$ ) in promoter regions, which is between 0 (unmethylated) and 1 (completely methylated). DMGs that showed  $|\Delta\beta|$  of 0.1 and adjusted p-value  $< 0.05$  were defined as significantly differentially methylated.

## Whole-genome mRNA microarray

Total RNA was extracted and purified with the mirVana™ miRNA Isolation Kit (Cat#AM1561, Ambion, USA) and subsequently amplified and labeled with the Low Input Quick Amp WT Labelling Kit (Cat#5190-2943, Agilent Technologies, Santa Clara, CA, US), following the manufacturer's instructions. RNA samples were then used to generate fluorescence-labelled cRNA targets for the SBC human ceRNA array V1.0 (4×180 K). The labelled cRNA targets were then hybridized and scanned on the Agilent Microarray Scanner (Agilent Technologies, USA). The data were extracted with Feature Extraction software 10.7 (Agilent Technologies, USA). Raw data were normalized by the Quantile algorithm using the *limma* package of R. The microarray experiments were performed according to the protocol of Agilent Technologies at Shanghai Biotechnology Corporation. Differential gene expression was determined using a t-test in the *limma* package. The fold change method was used to estimate the differential significance of genes. In this study, regrowth-related DEGs in 71 NFPA samples were defined as genes with an absolute fold change  $> 1.5$  or  $< 0.67$ , and p-value  $< 0.05$ .

## Integrating analysis

We integrated DNA methylation and gene expression by a two-step analysis process. First, we identified differentially promoter methylated and expressed genes in 20 regrowth and 51 non-regrowth patients. Second, for both differentially promoter methylated and differentially

expressed genes, we tested whether there is a strong association between DNA methylation and gene transcription. Pearson correlation analysis was used to assess the correlations. In this analysis, we applied the Pearson correlation coefficient (PCC) and p-value to investigate the correlation and significance between mRNA expression and DNA methylation with the function `cor.test` in R. A negative correlation was considered significant if  $PCC < -0.2$  and p-value  $< 0.05$ .

Functional enrichment analysis of Gene Ontology (GO) and Kyoto Encyclopedia of Genes and Genomes (KEGG) for target genes was performed to infer potential biological processes and pathways of regrowth-related genes using DAVID Bioinformatics Tool (version 6.8) [40]. The biological processes and pathways with a p-value  $< 0.05$  using the whole human genome as a reference were considered as significant functional categories.

## Survival analysis

The PFS analysis in our study was defined as the time from the surgery to the first diagnosis of regrowth. Patients with loss of follow-up or study end date were considered censored in the survival comparison analysis. Survival outcomes were estimated using the Kaplan-Meier method, and differences were tested using the log-rank test, and a p-value  $< 0.05$  was considered statistically significant.

## Development of regrowth related signature in NFPA

Candidate genes were integrated to form a regrowth-focus signature using a support vector machine with the sigmoid kernel to classify the regrowth and non-regrowth patients. An unbiased performance estimate in identifying regrowth patients was carried out using LOOCV. The diagnostic ability of the regrowth-focus prediction model was evaluated by obtaining the area under a receiver operating characteristic (ROC) curve. The ROC curve was produced by plotting true positive rates (sensitivity) against false positive rates (1-specificity). The permutation p-value of AUC was obtained from 1,000 randomization tests by randomizing mRNA expression data for testing the null hypothesis.

## Pyrosequencing assay

To validate the DNA methylation level of target genes in the promoter region, pyrosequencing assay was performed in another patient set ( $n = 12$ ). The DNA methylation level of target genes in the promoter region was assessed by pyrosequencing assay. Total DNA from tumour samples was extracted with a QIAamp DNA Mini Kit (Qiagen, Germany). For each

portion, 0.5 µg DNA was prepared to perform bisulfite conversion with EpiTect Bisulfite kit (Qiagen, Germany), according to the manufacturer's protocol. 1 µl of 10 µl eluted bisulfite converted DNA was prepared for PCR using a PyroMark PCR Kit (Qiagen, Germany), according to the manufacturer's instructions. The methylation level of the selected gene is measured as the percentage of average methylation in targeted CpG sites. The PCR primer used for the pyrosequencing assay was shown in Supplementary Table 7.

### **Real- time quantitative reverse transcription polymerase chain reaction (RT-PCR)**

Extraction and purification procedures of the tumour sample are the same as described above. Reverse transcription-PCR analyses were performed using the PrimerScript RT Reagent Kit (Takara, China). Quantitative real-time PCR was performed using LightCycler 480 SYBR Green I Master (Roche, Switzerland) with the ABI 9700 PCR system (Applied Biosystems, USA). The reaction steps were as follows: 95°C for 10 min followed by 40 cycles of 95°C for 10 s and 60°C for 30 s. The expression level was assessed by the standard curve method and normalized to the level of β-actin and was calculated using the  $2^{-\Delta\Delta ct}$  method [41]. The primer sequences are shown in Supplementary Table 8.

### **Statistical analysis**

All statistical analyses and modelling were performed in R (version 3.1) and IBM SPSS Statistics for Windows, version 21.0. The clinical characteristics were analysed with univariate and multivariate Cox regression analyses. Hazard ratio (HR) was calculated using Cox proportional hazards regression. The differences were considered to be statistically significant for  $p < 0.05$ .

### **Ethics approval**

This study was approved by the medical ethics committee of Beijing Tiantan Hospital.

### **Abbreviations**

PA: Pituitary adenoma; NFPA: Clinically non-functioning pituitary adenoma; PFS: Progress-free survival; PCC: Pearson correlation coefficient; SVM: Support vector machine; LOOCV: Leave one out cross-validation; ROC: Receiver operating characteristic; DMGs: Differentially methylated genes; DEGs: Differentially expressed genes; AUC: Area under the receiver operating characteristic curves.

## **AUTHOR CONTRIBUTIONS**

SC, CZL, WYX and YZZ were responsible for the research design. CZL, SC, YZM, JG and JCW were participated in the tumour sample preparation and clinical data collection. SC and WYX participated in performing the experiment. SC contributed to the manuscript writing and submission, statistical analyses and figure formatting. CZL, WYX, JCW and YZZ are responsible for funding application and management of the project. All authors have contributed to and approved the final manuscript.

## **ACKNOWLEDGMENTS**

We would like to thank Qiuyue Fang from Capital Medical University for the selfless assistance in performing experiments and collecting tumour samples.

## **CONFLICTS OF INTEREST**

The authors declare that they have no conflicts interests.

## **FUNDING**

This work was supported by grants from the National High Technology Research and Development Program of China (863 Program, 2014AA020610), National Natural Science Foundation of China (81771489, 81672495), Beijing Municipal Science & Technology Commission (Z171100000117002), Beijing Talents Fund (2015000021223ZK24) and China National Key Research and Development Program (2017YFC0908300), Xinjiang Uygur Autonomous Region Natural Science Fund Project (2018D01C092).

## **REFERENCES**

1. Ostrom QT, Gittleman H, Liao P, Vecchione-Koval T, Wolinsky Y, Kruchko C, Barnholtz-Sloan JS. CBTRUS Statistical Report: primary brain and other central nervous system tumors diagnosed in the United States in 2010-2014. *Neuro-oncol.* 2017 (suppl\_5); 19:v1–88. <https://doi.org/10.1093/neuonc/nox158> PMID:[29117289](https://pubmed.ncbi.nlm.nih.gov/29117289/)
2. Ebersold MJ, Quast LM, Laws ER Jr, Scheithauer B, Randall RV. Long-term results in transsphenoidal removal of nonfunctioning pituitary adenomas. *J Neurosurg.* 1986; 64:713–19. <https://doi.org/10.3171/jns.1986.64.5.0713> PMID:[3701419](https://pubmed.ncbi.nlm.nih.gov/3701419/)
3. Snyder PJ, Bashey HM, Phillips JL, Gennarelli TA. Comparison of hormonal secretory behavior of

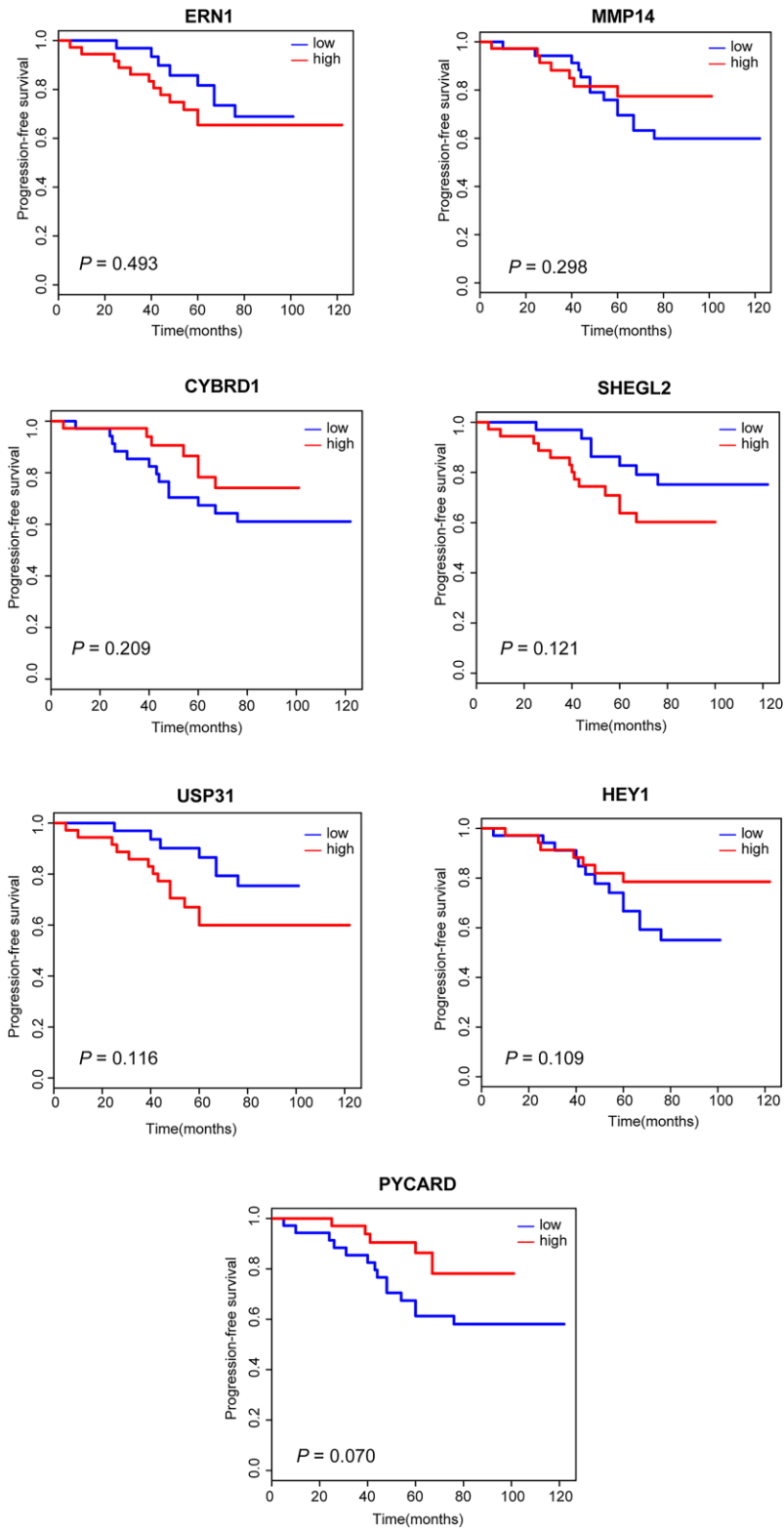
- gonadotroph cell adenomas in vivo and in culture. *J Clin Endocrinol Metab.* 1985; 61:1061–65.  
<https://doi.org/10.1210/jcem-61-6-1061>  
PMID:2414310
4. Brochier S, Galland F, Kujas M, Parker F, Gaillard S, Raftopoulos C, Young J, Alexopoulou O, Maiter D, Chanson P. Factors predicting relapse of nonfunctioning pituitary macroadenomas after neurosurgery: a study of 142 patients. *Eur J Endocrinol.* 2010; 163:193–200.  
<https://doi.org/10.1530/EJE-10-0255> PMID:20460423
  5. Li S, Yuan Y, Xiao H, Dai J, Ye Y, Zhang Q, Zhang Z, Jiang Y, Luo J, Hu J, Chen C, Wang G. Discovery and validation of DNA methylation markers for overall survival prognosis in patients with thymic epithelial tumors. *Clin Epigenetics.* 2019; 11:38.  
<https://doi.org/10.1186/s13148-019-0619-z>  
PMID:30832724
  6. Ding W, Chen G, Shi T. Integrative analysis identifies potential DNA methylation biomarkers for pan-cancer diagnosis and prognosis. *Epigenetics.* 2019; 14:67–80.  
<https://doi.org/10.1080/15592294.2019.1568178>  
PMID:30696380
  7. Wang Z, Kambhampati S, Cheng Y, Ma K, Simsek C, Tieu AH, Abraham JM, Liu X, Prasath V, Duncan M, Stark A, Trick A, Tsai HL, et al. Methylation Biomarker Panel Performance in EsophCap Cytology Samples for Diagnosing Barrett’s Esophagus: A Prospective Validation Study. *Clin Cancer Res.* 2019; 25:2127–35.  
<https://doi.org/10.1158/1078-0432.CCR-18-3696>  
PMID:30670490
  8. Koag MC, Kou Y, Ouzon-Shubeita H, Lee S. Transition-state destabilization reveals how human DNA polymerase  $\beta$  proceeds across the chemically unstable lesion N7-methylguanine. *Nucleic Acids Res.* 2014; 42:8755–66.  
<https://doi.org/10.1093/nar/gku554>  
PMID:24966350
  9. Kou Y, Koag MC, Lee S. Structural and Kinetic Studies of the Effect of Guanine N7 Alkylation and Metal Cofactors on DNA Replication. *Biochemistry.* 2018; 57:5105–16.  
<https://doi.org/10.1021/acs.biochem.8b00331>  
PMID:29957995
  10. Kou Y, Koag MC, Lee S. N7 methylation alters hydrogen-bonding patterns of guanine in duplex DNA. *J Am Chem Soc.* 2015; 137:14067–70.  
<https://doi.org/10.1021/jacs.5b10172>  
PMID:26517568
  11. Kober P, Boresowicz J, Rusetska N, Maksymowicz M, Goryca K, Kunicki J, Bonicki W, Siedlecki JA, Bujko M. DNA methylation profiling in nonfunctioning pituitary adenomas. *Mol Cell Endocrinol.* 2018; 473:194–204.  
<https://doi.org/10.1016/j.mce.2018.01.020>  
PMID:29410024
  12. Fukuoka H, Takahashi Y. The role of genetic and epigenetic changes in pituitary tumorigenesis. *Neurol Med Chir (Tokyo).* 2014; 54:943–57.  
<https://doi.org/10.2176/nmc.ra.2014-0184>  
PMID:25446387
  13. Gruppetta M, Formosa R, Falzon S, Ariff Scicluna S, Falzon E, Degeatano J, Vassallo J. Expression of cell cycle regulators and biomarkers of proliferation and regrowth in human pituitary adenomas. *Pituitary.* 2017; 20:358–71.  
<https://doi.org/10.1007/s11102-017-0803-0>  
PMID:28342098
  14. Yao X, Gao H, Li C, Wu L, Bai J, Wang J, Li Y, Zhang Y. Analysis of Ki67, HMGA1, MDM2, and RB expression in nonfunctioning pituitary adenomas. *J Neurooncol.* 2017; 132:199–206.  
<https://doi.org/10.1007/s11060-016-2365-9>  
PMID:28255749
  15. Noh TW, Jeong HJ, Lee MK, Kim TS, Kim SH, Lee EJ. Predicting recurrence of nonfunctioning pituitary adenomas. *J Clin Endocrinol Metab.* 2009; 94:4406–13.  
<https://doi.org/10.1210/jc.2009-0471> PMID:19820025
  16. Cheng S, Wu J, Li C, Li Y, Liu C, Li G, Li W, Hu S, Ying X, Zhang Y. Predicting the regrowth of clinically non-functioning pituitary adenoma with a statistical model. *J Transl Med.* 2019; 17:164.  
<https://doi.org/10.1186/s12967-019-1915-2>  
PMID:31109334
  17. Duong CV, Emes RD, Wessely F, Yacqub-Usman K, Clayton RN, Farrell WE. Quantitative, genome-wide analysis of the DNA methylome in sporadic pituitary adenomas. *Endocr Relat Cancer.* 2012; 19:805–16.  
<https://doi.org/10.1530/ERC-12-0251> PMID:23045325
  18. Simpson DJ, Hibberts NA, McNicol AM, Clayton RN, Farrell WE. Loss of pRb expression in pituitary adenomas is associated with methylation of the RB1 CpG island. *Cancer Res.* 2000; 60:1211–16.  
PMID:10728677
  19. Simpson DJ, Bicknell JE, McNicol AM, Clayton RN, Farrell WE. Hypermethylation of the p16/CDKN2A/MTS1 gene and loss of protein expression is associated with nonfunctional pituitary adenomas but not somatotrophinomas. *Genes Chromosomes Cancer.* 1999; 24:328–36.  
[https://doi.org/10.1002/\(SICI\)1098-2264\(199904\)24:4<328::AID-GCC6>3.0.CO;2-P](https://doi.org/10.1002/(SICI)1098-2264(199904)24:4<328::AID-GCC6>3.0.CO;2-P)  
PMID:10092131
  20. Bosch N, Cáceres M, Cardone MF, Carreras A, Ballana E, Rocchi M, Armengol L, Estivill X. Characterization and evolution of the novel gene family FAM90A in

- primates originated by multiple duplication and rearrangement events. *Hum Mol Genet.* 2007; 16:2572–82.  
<https://doi.org/10.1093/hmg/ddm209> PMID:17684299
21. Redon R, Ishikawa S, Fitch KR, Feuk L, Perry GH, Andrews TD, Fiegler H, Shapero MH, Carson AR, Chen W, Cho EK, Dallaire S, Freeman JL, et al. Global variation in copy number in the human genome. *Nature.* 2006; 444:444–54.  
<https://doi.org/10.1038/nature05329> PMID:17122850
  22. Salpea P, Russanova VR, Hirai TH, Sourlingas TG, Sekeri-Pataryas KE, Romero R, Epstein J, Howard BH. Postnatal development- and age-related changes in DNA-methylation patterns in the human genome. *Nucleic Acids Res.* 2012; 40:6477–94.  
<https://doi.org/10.1093/nar/gks312> PMID:22495928
  23. Day RN, Liu J, Sundmark V, Kawecki M, Berry D, Elsholtz HP. Selective inhibition of prolactin gene transcription by the ETS-2 repressor factor. *J Biol Chem.* 1998; 273:31909–15.  
<https://doi.org/10.1074/jbc.273.48.31909> PMID:9822660
  24. Fu L, Fu H, Wu Q, Pang Y, Xu K, Zhou L, Qiao J, Ke X, Xu K, Shi J. High expression of ETS2 predicts poor prognosis in acute myeloid leukemia and may guide treatment decisions. *J Transl Med.* 2017; 15:159.  
<https://doi.org/10.1186/s12967-017-1260-2> PMID:28724426
  25. Torres A, Alshalalfa M, Davicioni E, Gupta A, Yegnasubramanian S, Wheelan SJ, Epstein JI, De Marzo AM, Lotan TL. ETS2 is a prostate basal cell marker and is highly expressed in prostate cancers aberrantly expressing p63. *Prostate.* 2018; 78:896–904.  
<https://doi.org/10.1002/pros.23646> PMID:29761525
  26. Wallace JA, Li F, Balakrishnan S, Cantemir-Stone CZ, Pecot T, Martin C, Kladney RD, Sharma SM, Trimboli AJ, Fernandez SA, Yu L, Rosol TJ, Stromberg PC, et al. Ets2 in tumor fibroblasts promotes angiogenesis in breast cancer. *PLoS One.* 2013; 8:e71533.  
<https://doi.org/10.1371/journal.pone.0071533> PMID:23977064
  27. Zhang GW, Tian X, Li Y, Wang ZQ, Li XD, Zhu CY. Down-regulation of ETS2 inhibits the invasion and metastasis of renal cell carcinoma cells by inducing EMT via the PI3K/Akt signaling pathway. *Biomed Pharmacother.* 2018; 104:119–26.  
<https://doi.org/10.1016/j.biopha.2018.05.029> PMID:29772431
  28. He GH, Helbing CC, Wagner MJ, Sensen CW, Riabowol K. Phylogenetic analysis of the ING family of PHD finger proteins. *Mol Biol Evol.* 2005; 22:104–16.  
<https://doi.org/10.1093/molbev/msh256> PMID:15356280
  29. Kumamoto K, Fujita K, Kurotani R, Saito M, Unoki M, Hagiwara N, Shiga H, Bowman ED, Yanaihara N, Okamura S, Nagashima M, Miyamoto K, Takenoshita S, et al. ING2 is upregulated in colon cancer and increases invasion by enhanced MMP13 expression. *Int J Cancer.* 2009; 125:1306–15.  
<https://doi.org/10.1002/ijc.24437> PMID:19437536
  30. Li X, Kikuchi K, Takano Y. ING Genes Work as Tumor Suppressor Genes in the Carcinogenesis of Head and Neck Squamous Cell Carcinoma. *J Oncol.* 2011; 2011:963614.  
<https://doi.org/10.1155/2011/963614> PMID:21052543
  31. Walzak AA, Veldhoen N, Feng X, Riabowol K, Helbing CC. Expression profiles of mRNA transcript variants encoding the human inhibitor of growth tumor suppressor gene family in normal and neoplastic tissues. *Exp Cell Res.* 2008; 314:273–85.  
<https://doi.org/10.1016/j.yexcr.2007.07.029> PMID:17720155
  32. Ythier D, Brambilla E, Binet R, Nissou D, Vesin A, de Fraipont F, Moro-Sibilot D, Lantuejoul S, Brambilla C, Gazzeri S, Pedeux R. Expression of candidate tumor suppressor gene ING2 is lost in non-small cell lung carcinoma. *Lung Cancer.* 2010; 69:180–86.  
<https://doi.org/10.1016/j.lungcan.2009.11.006> PMID:19962781
  33. Lesage F, Guillemare E, Fink M, Duprat F, Lazdunski M, Romey G, Barhanin J. TWIK-1, a ubiquitous human weakly inward rectifying K<sup>+</sup> channel with a novel structure. *EMBO J.* 1996; 15:1004–11.  
<https://doi.org/10.1002/j.1460-2075.1996.tb00437.x> PMID:8605869
  34. Lesage F, Lauritzen I, Duprat F, Reyes R, Fink M, Heurteaux C, Lazdunski M. The structure, function and distribution of the mouse TWIK-1 K<sup>+</sup> channel. *FEBS Lett.* 1997; 402:28–32.  
[https://doi.org/10.1016/S0014-5793\(96\)01491-3](https://doi.org/10.1016/S0014-5793(96)01491-3) PMID:9013852
  35. Li Y, Zhang Z, Chen J, Liu W, Lai W, Liu B, Li X, Liu L, Xu S, Dong Q, Wang M, Duan X, Tan J, et al. Stella safeguards the oocyte methylome by preventing de novo methylation mediated by DNMT1. *Nature.* 2018; 564:136–40.  
<https://doi.org/10.1038/s41586-018-0751-5> PMID:30487604
  36. Zhang ZM, Lu R, Wang P, Yu Y, Chen D, Gao L, Liu S, Ji D, Rothbart SB, Wang Y, Wang GG, Song J. Structural basis for DNMT3A-mediated de novo DNA methylation. *Nature.* 2018; 554:387–91.  
<https://doi.org/10.1038/nature25477> PMID:29414941

37. Cury ML, Fernandes JC, Machado HR, Elias LL, Moreira AC, Castro M. Non-functioning pituitary adenomas: clinical feature, laboratorial and imaging assessment, therapeutic management and outcome. *Arq Bras Endocrinol Metabol.* 2009; 53:31–39.  
<https://doi.org/10.1590/S0004-27302009000100006>  
PMID:[19347183](https://pubmed.ncbi.nlm.nih.gov/19347183/)
38. Roelfsema F, Biermasz NR, Pereira AM. Clinical factors involved in the recurrence of pituitary adenomas after surgical remission: a structured review and meta-analysis. *Pituitary.* 2012; 15:71–83.  
<https://doi.org/10.1007/s11102-011-0347-7>  
PMID:[21918830](https://pubmed.ncbi.nlm.nih.gov/21918830/)
39. Losa M, Franzin A, Mangili F, Terreni MR, Barzagli R, Veglia F, Mortini P, Giovanelli M. Proliferation index of nonfunctioning pituitary adenomas: correlations with clinical characteristics and long-term follow-up results. *Neurosurgery.* 2000; 47:1313–18.  
<https://doi.org/10.1097/00006123-200012000-00009>  
PMID:[11126902](https://pubmed.ncbi.nlm.nih.gov/11126902/)
40. Huang W, Sherman BT, Lempicki RA. Systematic and integrative analysis of large gene lists using DAVID bioinformatics resources. *Nat Protoc.* 2009; 4:44–57.  
<https://doi.org/10.1038/nprot.2008.211>  
PMID:[19131956](https://pubmed.ncbi.nlm.nih.gov/19131956/)
41. Livak KJ, Schmittgen TD. Analysis of relative gene expression data using real-time quantitative PCR and the 2<sup>-</sup>(Delta Delta C(T)) Method. *Methods.* 2001; 25:402–08.  
<https://doi.org/10.1006/meth.2001.1262>  
PMID:[11846609](https://pubmed.ncbi.nlm.nih.gov/11846609/)

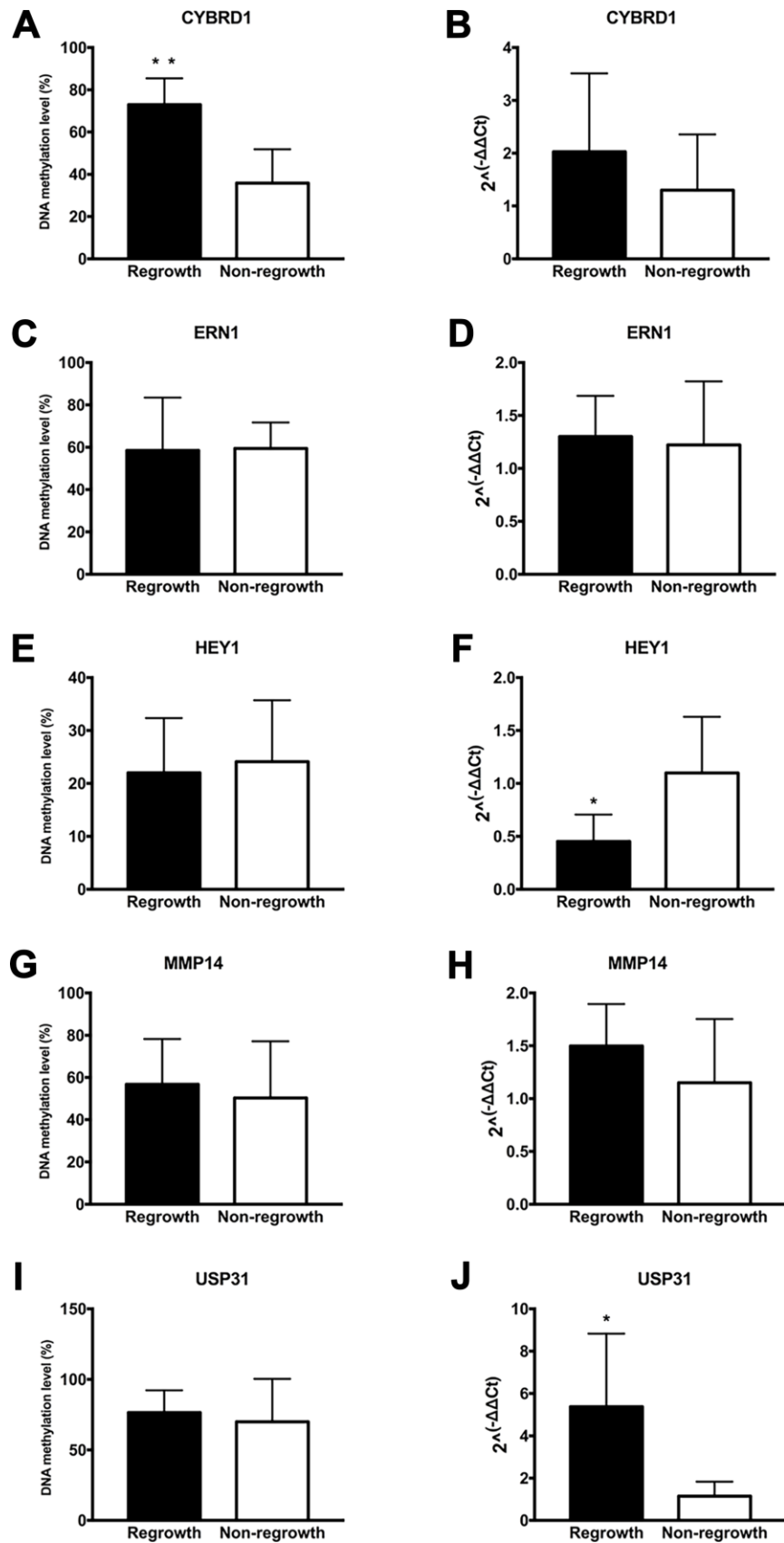
SUPPLEMENTARY MATERIALS

Supplementary Figures

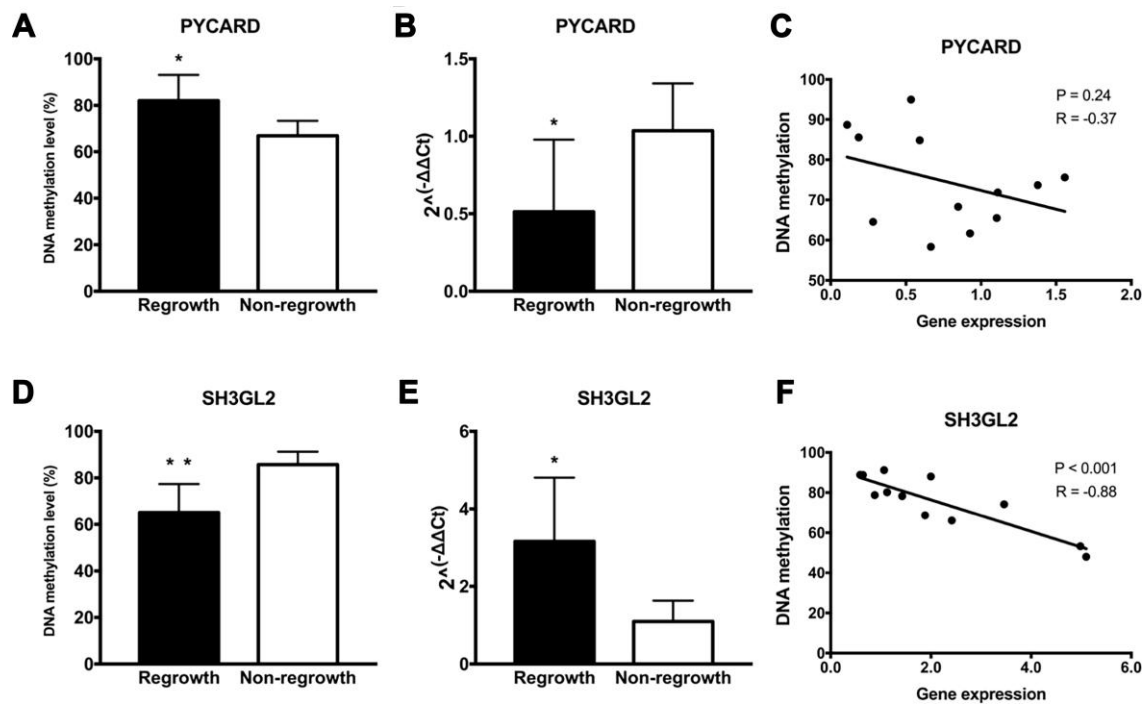


Supplementary Figure 1. Kaplan-Meier analyses of CYBRD1, ERN1, HEY1, MMP14 and PYCARD, in patients with NFPA.





**Supplementary Figure 2.** The DNA methylation status and expression levels of CYBRD1, ERN1, HEY1, MMP14 and PYCARD. \*  $p < 0.05$ , \*\*  $p < 0.01$ .



**Supplementary Figure 3.** The DNA methylation status, expression levels and Pearson correlation of SH3GL2 and USP31. Each dot represents average DNA methylation and gene expression level for every sample. \*  $p < 0.05$ , \*\*  $p < 0.01$ .

## Supplementary Tables

Please browse Full Text version to see the data of Supplementary Tables 1 to 6.

**Supplementary Table 1. Clinical information of 71 patients with NFPA.**

**Supplementary Table 2. List of differentially methylated genes.**

**Supplementary Table 3. List of differentially expressed genes.**

**Supplementary Table 4. Pearson analyses of 139 genes.**

**Supplementary Table 5. GO and KEGG analyses of 139 genes.**

**Supplementary Table 6. GO and KEGG analyses of 13 genes.**

**Supplementary Table 7. Pyrosequencing primers of 13 genes.**

No.	Gene	Forward primer	Reverse primer	Sequencing
1	FAM90A1	GGGTTAGGATGGGGTTTGA TTGGA	TCCCTCAAAAACCCTTTACCT TCAC	TTTGGGTTTGGGGTTA
2	MYT1L	GTGTTTTAATAAGATTGTA GGGAAAAGTT	CCATCATCATTATCTATAAAA CCATCTATT	GGGTAGGAATGATAAAT GTA
3	ETS2	AGGGTAAAGTGGAGATTAA ATTTTAGTTGA	ATCCATTCCTCATCATTCATA TTCT	TGAGTTTTTTATATAGTT TTTTGTG
4	ING2	GTGAAAGGAAATATGTGTT TTAAAGAA	ACAATAACTCCATCTTAACTC CCTACAAC	AAAAATTGTAAAGTTTG TTGG
5	STAT6	GTGGTTTAGAAGAGGGGGA ATTTT	ATCTCAACCCCTATCTACCC	TGTTGTAGAAGTTGAGA TTTTTTAG
6	KCNK1	ATGTTTTAGGGTTAGGTTAT TGTGTTAG	TCTTTCAAATTCCTCCCCTA TCC	TGAATGAAGGTAGAATT TTTTTAGT
7	CYBRD1	AGTGTTAAAAGTAAGTGGT GAGTA	TTACCTAATAACCTCACCCCTC TCC	ATTAGGTTTGTATTGA AGTT
8	ERN1	AGTTTGATGTTTGTGGGGA TTAATTAG	ATCCTCAATACTCACTTTTCT CTACA	GTTTTTTGGAAATTAGT GTG
9	HEY1	TGATTTGGTATAAGTTTTTT TGGGAATAA	ACCTTCTAAATCTTCCCCTCA T	AAAGTAAAATTAGTTGT TTTTATA
10	MMP14	TGGGTATTTAGAAGAGAGT AGTATTAATT	TTACCCCTCCTATCCTCCCCAA AAA	GGGGTAGTTAGGTTTTA G
11	PYCARD	GTTTGTGTTGTTTTGGGTTT GTATTAG	CTCTCTACCCTTTTATACAAC TCATTTT	ATAAAAACCAACCCAAA T
12	SH3GL2	GGGTTTTAGTAATTAATAA GAAATGATTAT	CCTTAATCAATATATCCCTCA ACATTC	GTGTAGGTTAGGTATAG TT
13	USP31	GATATTTTTTTGAGGTTTAT TTGAGATAGT	ACTATATATCAATCTACCCTA TCTATTCC	GTAATTTTTTTTTGTTTTA ATAAATA

**Supplementary Table 8. RT-PCR primers of 14 genes (including control).**

No.	Gene	Forward primer	Reverse primer	Product length(bp)	Ta(°C)
1	FAM90A1	TGAGAGCAGTGTTCGGAC	ACACACCTATTTACAAAGGGAT	107	60
2	MYT1L	GCCACCTAAAGATGGAGAAAT	CTCTAAGCTCTACTCCTGGTC	91	60
3	ETS2	ATAAACAGACATGTGACTGGG	CGTGGTTCAACCTCACATAC	81	60
4	ING2	CTGATATTTGAAGGGTAAGCAT	GAACTAGTCAATCTGCTGCC	89	60
5	STAT6	GCCAGCTTCCCTTCACTC	ATGGCTTAGGATCTATGACCC	67	60
6	KCNK1	AAAGTACATTGTGATTTGCAGC	CTGTTCATTTAGGGATTCGTG	71	60
7	CYBRD1	CTGATTGACCACAGTTGCC	TACAGTTTCCTGCTGGAGTTA	129	60
8	ERN1	TAGGCTGAGATGCACCAAG	CACCCTCTGAACTCCGTC	92	60
9	HEY1	AGCAGGTGTAGTTAAACGAC	ACAACACATCAGTACAACAGAG	63	60
10	MMP14	GAGAGTGAGACCCAGTGGA	CAGAAATCTAGCCGAACTGC	107	60
11	PYCARD	TAAGGGAGTCCCAGTCCTAC	AGGATGATTTGGTGGGATTG	102	60
12	SH3GL2	ATCATGTGGAGTGAAAGGC	ATTTATTGGAAACAGCGATGC	79	60
13	USP31	GGATAGTGATTTCTGTGTCGT	CTAGGAAAGACATCCTGCC	70	60
14	$\beta$ -actin	CATTCCAAATATGAGATGCGTT	TACACGAAAGCAATGCTATCAC	133	60